# On the Feasibility of the Multipath Fingerprint Method for Location Finding in Urban Environments

Ivy Y. Kelly, Hai Deng and Hao Ling

Department of Electrical and Computer Engineering
The University of Texas at Austin
Austin, TX 78712-1084

**Abstract**

The feasibility of the multipath fingerprint method for wireless location finding in urban environments is examined using computational electromagnetics simulation. Fingerprints composed of time and angle of arrival data in urban environments are created using electromagnetic ray tracing. The fingerprints at specific locations within a simple four-by-four building model are studied to address issues including uniqueness of the fingerprints, repeatability due to environmental changes, and bandwidth limitations. A classifier based on template matching is also constructed using the simulation data from a 1-km city area of downtown Austin, Texas. Angle of Arrival (AOA) is found to be a stronger identifier than Time of Arrival (TOA). The classifier results demonstrate that good location-finding performance is achievable using both time of arrival and angle of arrival features.

## 1. Introduction

By October 2001, wireless callers to the emergency number 911 must be located within 125 meters of their actual positions, according to regulations contained in the Federal Communications Commission (FCC) Docket 94-102 [1, 2]. There are many other uses for wireless location finding including location-sensitive billing, intelligent transport systems (ITS), and electronic yellow pages [3 - 5]. However, the Docket 94-102 regulations have been the major impetus behind the strong recent interest in location finding.

The best-known location finding methods are GPS (Global Position System), AOA, and TDOA (Time Difference of Arrival). Each of these solutions has advantages and disadvantages. GPS is a handset solution (i.e., modifications are made to the handset) that is well-tested and very accurate except in urban canyons where one or more of the necessary satellites are blocked [4, 6]. AOA and TDOA are network solutions (i.e., modifications are needed at the base stations only) that require two or three base stations to identify a location [6]. However, a direct line of sight (LOS) signal is needed at all base stations to properly locate a caller. Similar to the GPS solution, urban environments pose a problem to these methods since LOS is very uncommon and the propagation channels are dominated by multipath.

One proposed method that can potentially work well in an urban setting is the multipath fingerprint method [7]. It is a network-based solution that actually takes advantage of the multipath information in the incoming signal to identify the location of the mobile user. It does not require a LOS signal and only uses one base station. The basic idea of the method is to extract the features of the multipath signals contained in the incoming call, including the parameters of angle of arrival ($\theta$), time delay ($\tau$), and signal strength ($\gamma$). The bandwidth of the incoming signal is used to extract time delay. Angle of arrival is extracted by using an antenna array at the base station. The three parameters from all the multipath components of the signal are used to create a fingerprint that is compared to a database of fingerprints previously cataloged. Each fingerprint in the database corresponds to a known location. Thus, when a matching fingerprint is found in the database, the correct location is found as well (Figure 1).

In this paper, we carry out a study to examine the feasibility of the multipath fingerprint method. The data for our study is based on channel data simulated by applying electromagnetic ray tracing to urban CAD models [8]. The ray-based simulation allows us to accurately extract the required parameters and to pinpoint the cause-and-

effect between the physical propagation mechanisms and the resulting features. We study the fingerprints in the database at specific locations within the urban environment to address issues including the uniqueness of the fingerprints, repeatability due to environmental changes, and bandwidth limitations. In addition, we construct a classifier based on template matching using the simulation data from a 1-km city area to more closely investigate the location-finding performance of the fingerprinting approach.

This paper is organized as follows. Section 2 describes the ray tracing simulation used to generate the channel data and the methodology used to construct the simulation database. Section 3 describes results and findings from a simple four-by-four building model. In Section 4, we construct a classifier based on the simulation results generated using a CAD model of downtown Austin, Texas and evaluate the performance of the multipath fingerprint scheme. Discussions and conclusions are given in Section 5.

## 2. Ray Tracing Simulation for Fingerprint Generation

We first generate the necessary channel data for this study using a code called CPATCH, which is an electromagnetic ray tracer designed for telecommunications applications [9]. It calculates the coupling between transmitting and receiving antennas in a complex environment by using the shooting and bouncing ray (SBR) technique [10, 11]. Rays are shot in all angular directions from the transmitter location and traced according to the laws of geometrical optics as they bounce around in a CAD model description of the environment. The phase of the field along each ray is calculated by tracking the total distance traveled by the ray as well as the phase change due to reflections. The amplitude is computed by taking into consideration the antenna pattern, the divergence of the ray tube, field polarization and the materials used in the model. The field at the receiving antenna is then computed by summing the contributions from all the ray tubes that illuminate the receiver location.

In actual implementation, a grid of receiver locations is first defined and each receiver location is updated as each ray is traced. Since only the receiver points within the ray tube are updated for each ray, the total computation time is essentially independent of the number of receiver points. The majority of the computation time is the ray tracing time. For a CAD model of an $8 \times 10$ block area of a city containing over 21,000 triangular facets, the simulation time is less than 10 minutes on a typical workstation. Channel characteristics simulated using this approach have been compared against measurement data in Austin, Texas and the results showed fairly good agreement between simulation and measurement [12].

The CPATCH methodology described above is well suited for calculating the channel data from a fixed transmitter to a large number of receiver locations. However, the problem at hand is to simulate the multipath fingerprints from handset transmission at multiple locations to a fixed base station receiver. In order to effectively simulate the fingerprint data needed in this study, we invoke reciprocity [13]. We first perform ray tracing from the base station assuming it is the transmitter. For each handset location, we find all the rays that contribute to that particular location. Then based on reciprocity, we assume those rays are also the ones that will reach the base station receiver if the handset is used as the transmitter. Next, the parameters needed to form a fingerprint are readily extracted from the information for each ray. The time of arrival is directly proportional to the total disance travel by the ray. The signal strength is proportional to the field strength of the ray. The angle of arrival at the base station is obtained from the ray direction with respect to the base station. Therefore, using only a one-time ray trace, we can obtain the needed multipath fingerprint information for all possible handset locations.

## 3. Phenomenology Study of a Simple Model

We first investigate the characteristic features of the fingerprints using a simple model consisting of 16 buildings in a symmetrical four-by-four arrangement. The center frequency is chosen at 1.0 GHz. The buildings are identical with 30 meters in height, width, and length, and are placed 30 meters apart on a square grid (Figure 2a). All surfaces are assumed to be perfectly conducting. A base station antenna is placed in the middle of the model at a height of 15 meters above ground. Fingerprints are examined for each 30-meters-by-30-meters sector, located between each of the buildings (Figure 2b). To form the fingerprints within each sector, we collect 9 fingerprints from 9 mobile locations, each 10 meters apart. Fingerprints are formed from the angle of arrival, time delay, and signal strength data as calculated by CPATCH. The individual fingerprints from each of the 9 mobile locations are summed to form a fingerprint template (called Mx) for that sector. Data for a total of 65 sectors are generated.

Figure 3 shows the fingerprint templates from Sectors 5, 12, 19, and 26, which make up half of a typical LOS street. Each template on a LOS street has a unique feature, an arc from the LOS rays. The arc is centered around 90° in each of the four fingerprint templates shown. The arc gets narrower and is located at a larger time of arrival (TOA) as the location of the sector gets farther from the base station. Although not shown, the arc is shifted by 180° on the other side of the base station on the same street. In fact, it is found that angle of arrival (AOA) is the main distinguishing feature between different quadrants of the model. Although the model is perfectly symmetrical, each of the four quadrants has features that are 90° shifted from the quadrant next to it.

The fingerprint templates from Sectors 3, 11, 17, and 25 are shown in Figure 4. These sectors make up half of the street immediately parallel to the LOS street from Figure 3. Sector 3 is the farthest from the base station. Each of the three most prominent features in Sector 3 can be seen in the other three sectors at the same AOA. The TOA, of course, decreases as the location of the sector gets closer to the base station. Finally, fingerprint templates from Sectors 1, 10, 15 and 24 (i.e., the street parallel to the previous two streets and farthest from the base station) have fewer features. This is due to the limitation of the simulation, as we have chosen to terminate the ray tracing for any ray that exceeds 5 bounces. For this reason, the outermost sectors have few features. In a larger environment (e.g. Austin, TX, which will be studied next), more bounces are included in the calculations to provide features in sectors farther from the base station.

In order to examine the uniqueness of the fingerprints at different locations in this model, we calculate the correlation coefficient between the fingerprint templates from different sectors. For this calculation, we assume that the AOA is known on an absolute angular scale, while the time origin of the TOA is not known. In practice, the AOA will be extracted from an antenna array at the base station. Therefore, it is reasonable to assume that absolute AOA can be determined (e.g., using a circular array). However, the time origin of the TOA will not in general be known since the handset and base station are not synchronized with the precise time of call origination. We implement the correlation calculation using a one-dimensional Fourier transform along the TOA axis and use the peak value to give a measure of how well one fingerprint correlates with another.

Figure 5a shows the correlation coefficient matrix for each fingerprint template with every other fingerprint template in the database. The correlation coefficient is normalized to take on a value between zero and one. The diagonal values of the correlation coefficient matrix are '1', since each fingerprint correlates perfectly with itself. The off-diagonal terms represent the possible confusion amongst the fingerprints. Figure 5b shows the center 9x9 portion of the correlation matrix that corresponds to Sectors 29-37 along the horizontal LOS street. The block-diagonal structure can be understood since the templates along each side of the LOS street share the same arc feature shown in Figure 3a. Since the features on opposite sides of the LOS street are 180° off from each other, fingerprints on the same side of the street have a stronger correlation. The TOA information becomes the main distinguishing features in the templates for these sectors. Figure 5c shows the portion of the correlation matrix that corresponds to Sectors 15-23 along the next parallel street. The fingerprints farthest from the base station are most highly correlated since they contain the least amount of features and those features have similar AOA.

Next, we study the effect of finite frequency bandwidth and array size on the correlation matrix. Contrary to the present simulation data, there are resolution limits due to frequency bandwidth and array size on how well the fingerprint features can be extracted in practice. The smaller the frequency bandwidth and the array size, the more difficult it is to resolve the TOA and AOA. Figure 6a is the correlation coefficient matrix of ten of the sectors (Sectors 34, 35, 36, 37, 41, 48, 49, 50, 51 and 55) in the lower right quadrant formed from the original simulation data. These ten fingerprint templates are low-pass filtered to correspond to a frequency bandwidth of 2.9MHz and an array size of 0.6m. Figure 6b is the correlation coefficient matrix of these ten templates after the low pass. As expected, the cross correlation levels increase, making the correct identification of fingerprints more difficult.

Finally, we consider the fluctuation of the fingerprints due to changes in the environment. For this study, we examine the fingerprints with the addition of cars on the streets. The car CAD model is designed with specifications from a Ford Mustang Coupe and a Ford Escort Sedan [14]. Sixty-five fingerprint templates are created in the four-by-four model in the same locations as before, but by including 190 cars in the lower right-hand quadrant. The cars are placed in Sectors 34, 36, 41, 42, 48, 50, 55, and 56 to simulate parked cars along the buildings as well as traffic in the streets (Figure 7). A new set of correlation coefficients is calculated by comparing the new fingerprint templates with cars to the original template database without cars. Figures 8a to 8c show three examples of this comparison between the new correlation and the original correlation values for Sectors 34, 41 and

48, respectively. The dotted line is the new correlation between the fingerprint template with cars and the 65 original fingerprint templates without cars. The solid line shows the original correlation values with no cars. These three sectors (34, 41 and 48) contain the most noticeable differences in the correlation coefficients. As can be seen, the addition of traffic causes very little change in the correlation.

## 4. Classifying Results in an Urban Setting

To more directly investigate the location-finding performance of the multipath fingerprint approach, we construct a classifier based on template matching by using the simulation data at 1.0 GHz from a 1-km city area. We set out to determine the probability of correctly identifying the unknown handset location using its AOA-TOA fingerprint, when a database of known fingerprints is available. The urban area examined is based on a CAD model of the city of Austin, Texas, obtained from a local architectural firm (Figure 9). This model is significantly more complex than the four-by-four model studied in the last section. Since the requirement for wireless E-911 location finding is 125 meters, the downtown area is first divided into 7x8=56 sectors, as shown in Figure 10. Each sector is a square of size 125 m x 125 m. The base station is located at the intersection of Congress Avenue and 7$^{th}$ Street, in Sector 25. Fingerprints are calculated using CPATCH at multiple handset locations on the streets within each sector. On average, there are about 180 such locations within each sector. We denote each sample fingerprint by a 2-D intensity image, $R_k(m,n)$, where $m$ is the TOA index and $n$ is the AOA index. The resolution interval in the TOA dimension is chosen to be 800ns. This corresponds to a frequency bandwidth of 1.25 MHz, which is typical of a channel in a CDMA system. The resolution interval in the AOA dimension is chosen to be 5°. This corresponds to an array of dimension 12 wavelengths. The size of the resulting fingerprint images is 100×72.

We randomly choose $L$=40 locations in a sector and form a template for the classification database by averaging the individual fingerprints. The template for sector $j$ is constructed simply as an average of the individual fingerprints:

$$T_j(m,n) = \frac{1}{L}\sum_{k\in j} R_k(m,n) \tag{1}$$

Next, we define the match score between an individual fingerprint image $R(m,n)$, and the template for sector $j$, $T_j(m,n)$. Since the received signal amplitude changes dramatically with propagation distance, a correlation score is chosen instead of the mean squared error criterion. Our match score definition is [15-17]:

$$\text{Match Score}_j = \max_p \frac{\sum_m \sum_n R^l(m,n) T_j^l(p-m,-n)}{\sqrt{\sum_m \sum_n R^{2l}(m,n) \sum_m \sum_n T_j^{2l}(p-m,-n)}} \tag{2}$$

This match score is normalized by the signal energy so that it takes on values between zero and one. As has been discussed in the last section, the correlation process is only carried out in the TOA dimension due to the lack of a time reference. Note also that we apply a power transform (where $l$ is the power transform parameter) to both the individual fingerprint and the template. Usually we choose $l$ to be a small number (0.02) to emphasize the weaker features that might be important in the matching process.

With the templates computed using in (1) and the correlation match score defined in (2), we set out to find the correct location-finding probability, $P_{lf}$, for the fingerprints generated in each sector. We experimentally determine $P_{lf}$ for each sector by feeding a large number of test fingerprints to the template-matching process in (2). For each fingerprint tested, the sector with the highest match score is identified as the location of the handset. The forced decision rule is used, i.e., the sector with the highest match score is chosen no matter how low the score. Finally, after all the test fingerprints have been identified, we tally up the number of correct identifications relative to the total number of test fingerprints to arrive at $P_{lf}$.

Table 1 shows the results of the location finding for all 56 sectors in the downtown Austin area. Each block in the table denotes a sector. The first number is the index of the sector. The second number is the correct sector location-finding probability ($P_{lf}$). We observe that for most of the sectors, $P_{lf}$ is greater than 70%. The

average $P_{lf}$ for all sectors is 76%. However, for a few sectors it is below 30% (Sectors 48, 51, 55). Closer examination of the fingerprints in these sectors reveals that either there are fewer features within these sectors, or the features are similar to the adjacent sectors. We also compute the probability of successfully identifying either the correct sector or the sectors immediately adjacent to the correct sector. For those interior sectors, this includes 8 adjacent sectors. For the border sectors, this includes either 5 or 3 (corners) adjacent sectors. This probability, $P_{alf}$, is shown as the third number in each sector in Table 1. We observe that $P_{alf}$ is in general much higher than $P_{lf}$, especially for those sectors where $P_{lf}$ is low. The average $P_{alf}$ is found to be 92%. Therefore, when misidentifications occur in the classification process, the fingerprint locations tend to be misidentified in an adjacent sector. In practice, this is certainly not as detrimental as when the handset location is misidentified in a sector very far away from its true location.

Next we investigate the relative importance of the AOA features and the TOA features. Table 2 shows the correct location finding probabilities obtained using AOA information only. For AOA-only processing, the 1-D fingerprints are matched against the 1-D templates, with the same set of parameters as the 2-D processing. The average probabilities of correct identification are found to be $P_{lf}$ = 60% and $P_{alf}$ = 80%. Table 3 shows the correct location finding probabilities obtained using TOA information only. In this case, a 1-D correlation operation with time-shift is applied in the matching process. The average probabilities of correct identification are found to be $P_{lf}$ = 24% and $P_{alf}$ = 40%. Clearly, due to the lack of a time reference, the performance of the TOA-only classifier is much worse than that of the AOA-only classifier. The 2-D fingerprint processing results are significantly improved compared with 1-D processing results in either case.

Lastly, we consider the effect of inaccuracies in the AOA and TOA positions on the performance of location finding. While in this simulation study we have assumed that the fingerprint features are readily available, in the actual implementation, the 2-D features must be extracted from the incoming handset signal prior to the classification process. The accuracy with which the AOA and TOA positions can be extracted from the incoming handset signal depends on, respectively, the size of the base station array and the frequency bandwidth of the signal. We simulate the inaccuracies by adding Gaussian jitters with standard deviation of one fourth of the resolution cell to the AOA and TOA positions of the individual test fingerprints. The templates in the database remain unperturbed. Table 4 shows the performance of the 2-D fingerprint classifier with corrupted features. The average probabilities of correct identification are found to be $P_{lf}$ = 71% and $P_{alf}$ = 88%. Compared to the results from Table 1 ($P_{lf}$ = 76% and $P_{alf}$ = 92%), the performance of the corrupted data is only slightly worse than that of the uncorrupted data. This implies that the needed accuracy for the feature extraction algorithm should be on the order of one-half the Fourier resolution. This appears to be within the reach of parameter estimation algorithms such as MUSIC.

## 5. Conclusions

In this paper, we have applied computational electromagnetics simulation to examine the feasibility of the multipath fingerprint method as a wireless location-finding tool in urban areas. The electromagnetics simulation was carried out using ray tracing, which allowed us to accurately extract the time of arrival and angle of arrival features used to form the fingerprints. Results from a four-by-four building model showed that fingerprints are quite unique at various locations even in such a highly symmetrical environment. Repeatability was examined by simulating traffic in the simple model. Bandwidth effects were studied to show the effect due to frequency bandwidth and finite array size. In addition, we have constructed a classifier based on template matching using the simulation data from a 1-km city area of downtown Austin, Texas to more directly investigate the location-finding performance of the fingerprinting approach. AOA was shown to be a stronger identifier than TOA. The classifier results demonstrated that good location finding performance is achievable using both AOA and TOA features. Also studied was the effect of errors in the AOA and TOA features on the classifier performance. We believe that the main challenge in the implementation of such a system is how to reliably and accurately extract the AOA and TOA features from noisy, band-limited data.

## 6. Acknowledgments

The authors would like to thank Drs. Arthur Giordano and Samuel Rescheff, and the Wireless Access Technologies Department in the Network Infrastructure Lab at GTE Laboratories, Inc. for their support and assistance in this research. The authors would also like to thank SAIC-Demaco of Champaign, IL for supplying the

CPATCH code used in this study. This work is supported in part by the Texas Higher Education Coordinating Board under the Texas Advanced Technology Program.

## 7. References

[1] "FCC Adopts Rules to Implement Enhanced 911 for Wireless Service," FCC News, CC docket no. 94-102, June 12, 1996

[2] FCC Docket 94-102, "Report and Order and Further Notice of Proposed Rulemaking in the Matter of Revision of the Commission's Rules to Ensure Compatibility with Enhanced 911 Emergency Calling Systems," stated June 12, 1996; published July 26, 1996.

[3] C. Drane, M. Macnaughtan and C. Scott, "Positioning GSM Telephones," *IEEE Communications Magazine,* vol. 36, no. 4, pp. 46-59, Apr. 1998.

[4] M. Licht, "Tracking Emergency Calls," WB&T, p 29-30, Apr. 1998.

[5] J.Caffery, Jr. and G. Stuber, "Overview of Radiolocation in CDMA Cellular Systems," *IEEE Communications Magazine,* vol. 36, no. 4, pp. 38-45, Apr. 1998.

[6] J. Reed, K. Krizman, B. Worener and T. Rappaport, "An Overview of the Challenges and Progress in Meeting the E-911 Requirement for Location Service," *IEEE Communications Magazine,* vol. 36, no. 4, pp. 30-37, Apr. 1998.

[7] M.Wax and A. Leshem, "Joint Estimation of Time Delays and Directions of Arrival of Multiple Reflections of a Known Signal," *IEEE Transactions on Signal Processing*, vol. 45, no. 10, p. 2477-2484, Oct. 1997.

[8] I.Y. Kelly, H. Ling, and W.J. Vogel, "Urban Channel Propagation Modeling Using the Shooting and Bouncing Ray Technique," to appear in *Microwave and Optical Technology Letters*, Mar. 2000.

[9] S.W. Lee, J.E. Baldauf and R. A. Kipp, "CPATCH: Antenna Coupling in Complex Environments," DEMACO Tech. Rep., Champaign, IL, Oct. 1994.

[10] H. Ling, R. Chou and S.W. Lee, "Shooting and Bouncing Rays: Calculating the RCS of an Arbitrarily Shaped Cavity," *IEEE Transactions on Antennas and Propagation*, vol. 37, no. 2, pp. 194-205, Feb. 1989.

[11] S.W. Lee, H. Ling and R. Chou, "Ray-Tube Integration in Shooting and Bouncing Ray Method," *Microwave and Optical Technology Letters*, vol. 1, no. 8, pp. 286-289, Oct. 1988.

[12] G. Benavides, "A Fast Algorithm to Calculate Channel Characteristics of an Urban Environment," masters thesis, University of Texas at Austin, Austin, TX, 1998.

[13] C. Balanis, *Antenna Theory Analysis and Design*, New York: John Wiley & Sons, 1982.

[14] Web site for Ford Motor Company, http://www.ford.com

[15] R. Duda and P. Hart, *Pattern Classification and Scene analysis,* New York: John Wiley & Sons, 1973.S.

[16] Hudson, "Correlation Filters for Aircraft Identification from Radar Range Profiles," *IEEE Transactions on Aerospace and Electronic Systems*, vol. 29, no. 3, pp. 741-749, July 1997.

[17] T. D. Ross, S. W. Worrell, V. J. Velten, J. C. Mossing and M. L. Bryant, "Standard SAR ATR Evaluation Experiments Using the MSTAR Public Release Data Set," *Proceedings of SPIE*, Algorithm for SAR Imagery V, vol. 3370, pp. 566-573, April 1998.

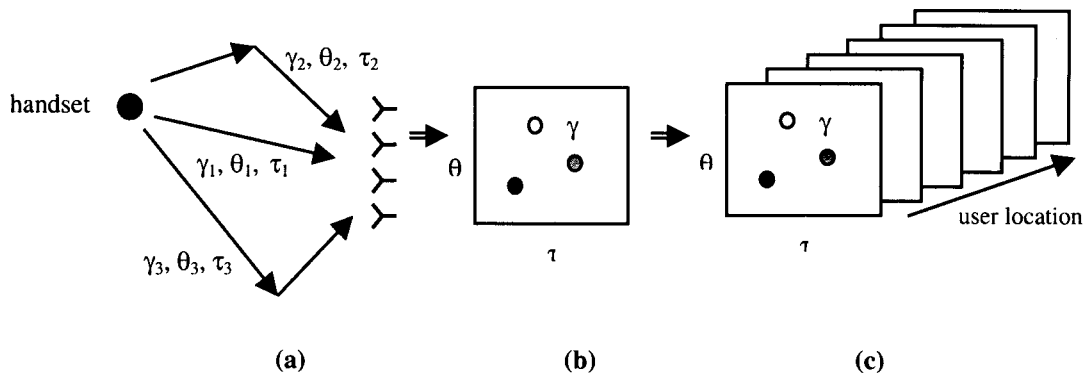


**Figure 1. Multipath Fingerprint System.**
**(a) Multipath components of the handset signal arriving at the base station.**
**(b) Fingerprint created from parameters extracted from the incoming signal.**
**(c) Existing fingerprint database – each fingerprint is associated with a specific mobile location. The extracted fingerprint from the handset signal is compared to the database to find the best fingerprint match and thus the handset location.**

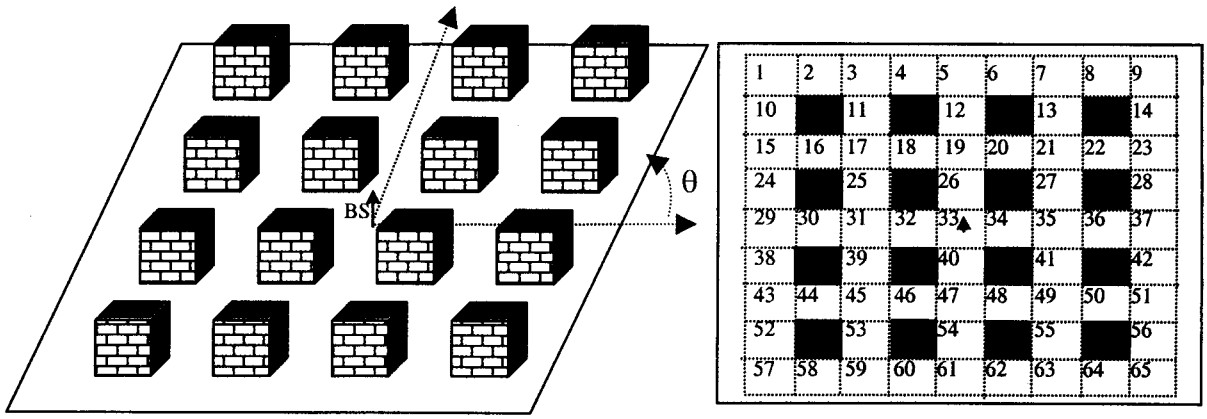


**Figure 2. Four-by-four symmetrical building model.**

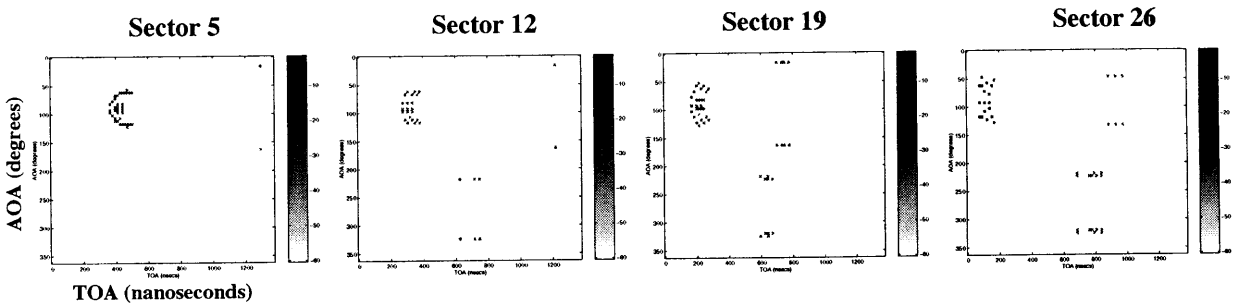


**Figure 3. Fingerprints for the sectors along the LOS street in the four-by-four symmetrical model.**

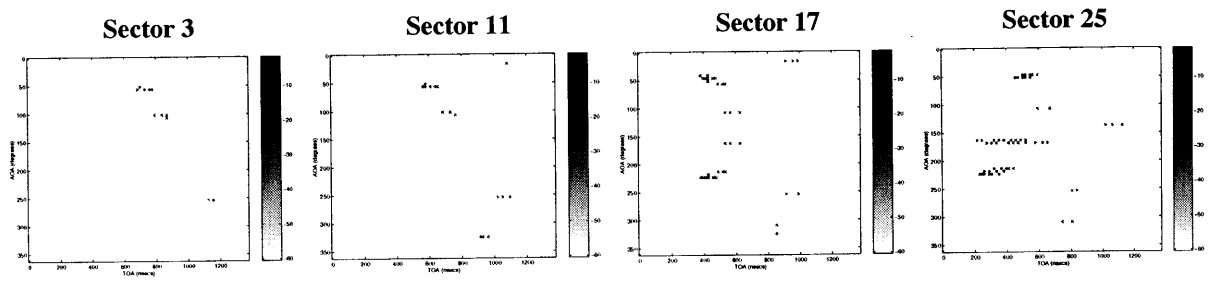


**Figure 4. Fingerprints for the sectors along the non-LOS parallel street in the four-by-four symmetrical model.**

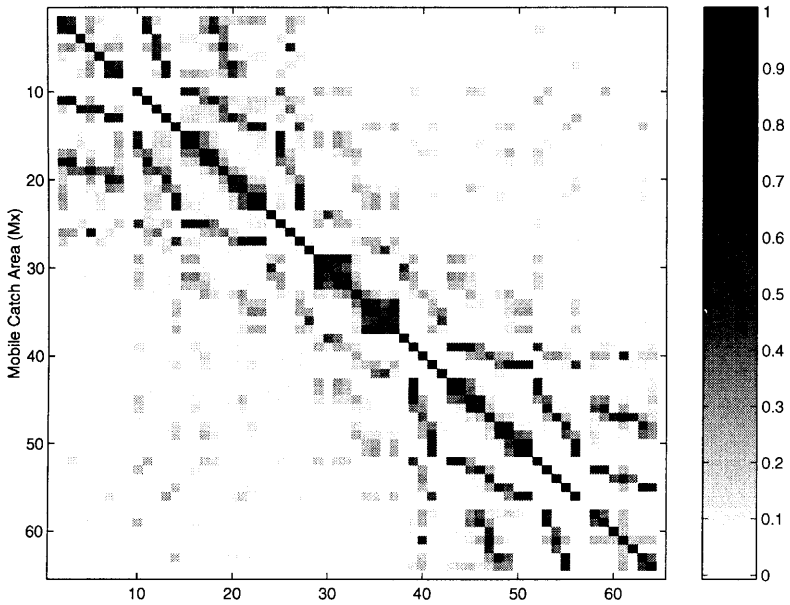


**Figure 5a. Correlation coefficient matrix for all the fingerprints in the four-by-four model.**

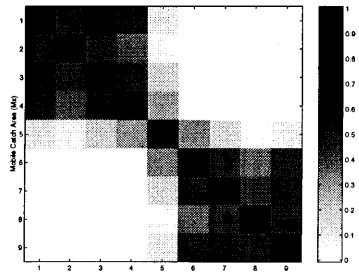

**Figure 5b. LOS street, Sectors 29-37**

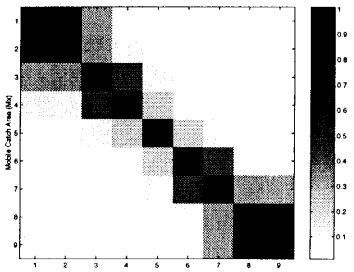

**Figure 5c. Parallel Street, Sectors 15-23**

**Figure 5. Correlation coefficient matrix for the four-by-four model.**

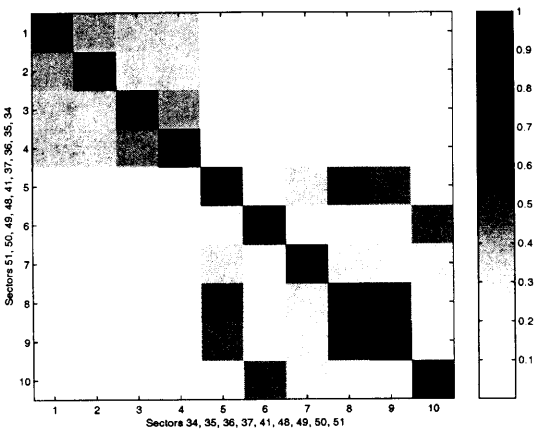


Figure 6a. Correlation Coefficient Matrix for Mx34, 35, 36, 37, 41, 48, 49, 50, 51, 55 assuming infinite AOA and TOA resolution

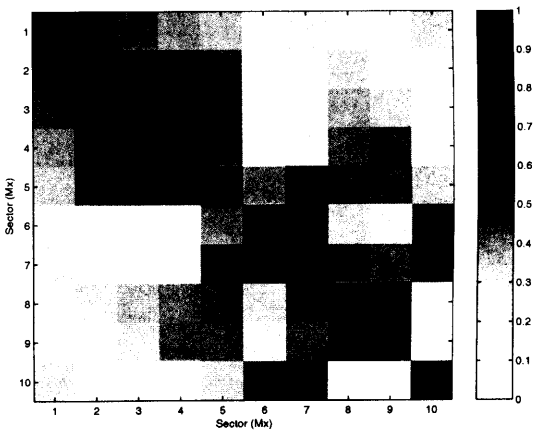


Figure 6b. Correlation Coefficient Matrix with 2.9 MHz bandwidth and array size 2λ

**Figure 6. Correlation coefficient matrix for the lower right-hand quadrant showing the effect of limited bandwidth and array size.**

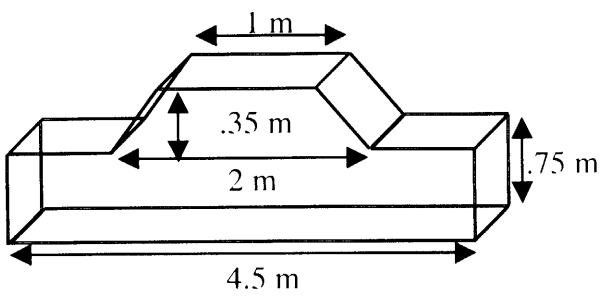


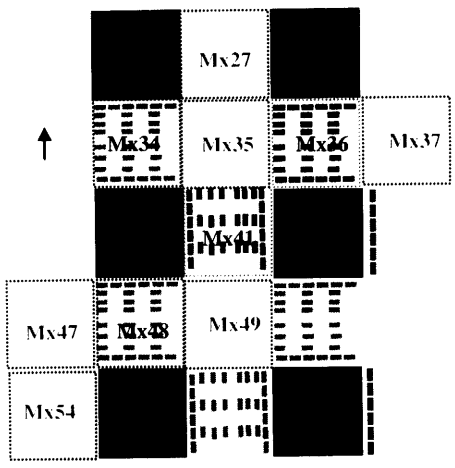


**Figure 7. Car model and location of cars placed in the four-by-four model.**

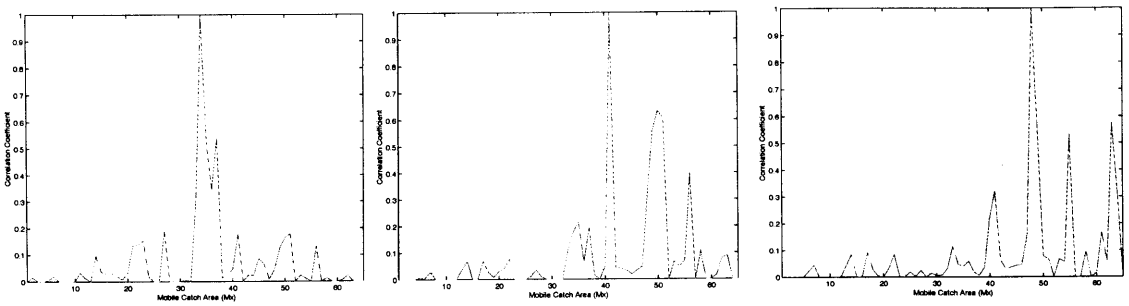

Figure 8a. Mx34 Figure 8b. Mx41 Figure 8c. Mx48

**Figure 8. Effect of cars on the correlation coefficient.**
**Solid, Blue - original template without cars compared to database.**
**Dotted Red - template with cars compared to database**


**Figure 9. CAD model of dowtown Austin, Texas.**

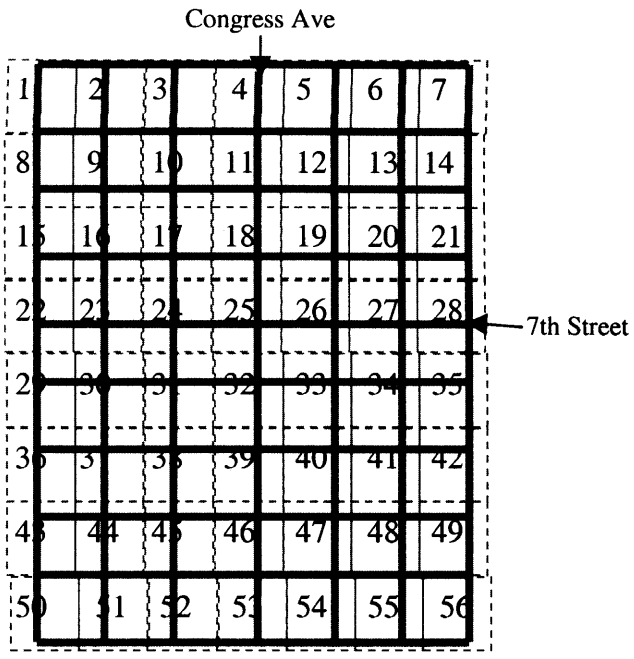


**Figure 10. Sectorization of dowtown Austin, Texas.**

| 1 | 2 | 3 | 4 | 5 | 6 | 7 |
|---|---|---|---|---|---|---|
| 0.95 | 0.73 | 0.82 | 0.86 | 0.78 | 0.82 | 0.88 |
| 0.95 | 0.88 | 0.95 | 0.98 | 0.98 | 0.91 | 0.89 |
| 8 | 9 | 10 | 11 | 12 | 13 | 14 |
| 0.84 | 0.67 | 0.87 | 0.92 | 0.95 | 0.89 | 0.91 |
| 0.85 | 1 | 0.97 | 1 | 0.97 | 1 | 0.91 |
| 15 | 16 | 17 | 18 | 19 | 20 | 21 |
| 0.92 | 0.76 | 0.82 | 0.69 | 0.97 | 0.82 | 0.83 |
| 0.99 | 0.93 | 0.9 | 0.98 | 1 | 0.92 | 0.87 |
| 22 | 23 | 24 | 25 | 26 | 27 | 28 |
| 0.99 | 0.57 | 0.62 | 0.68 | 0.9 | 0.88 | 1 |
| 0.99 | 0.96 | 0.81 | 0.84 | 0.96 | 1 | 1 |
| 29 | 30 | 31 | 32 | 33 | 34 | 35 |
| 0.85 | 0.81 | 0.74 | 0.82 | 0.76 | 0.79 | 0.87 |
| 0.9 | 0.96 | 0.82 | 0.86 | 0.82 | 0.94 | 0.99 |
| 36 | 37 | 38 | 39 | 40 | 41 | 42 |
| 0.54 | 0.65 | 0.62 | 0.63 | 0.7 | 0.62 | 0.9 |
| 0.81 | 0.93 | 0.83 | 0.88 | 0.88 | 0.91 | 0.96 |
| 43 | 44 | 45 | 46 | 47 | 48 | 49 |
| 1 | 0.35 | 0.52 | 0.7 | 0.56 | 0.22 | 0.89 |
| 1 | 0.94 | 0.85 | 0.94 | 0.88 | 1 | 1 |
| 50 | 51 | 52 | 53 | 54 | 55 | 56 |
| 0.87 | 0.24 | 0.53 | 0.87 | 0.6 | 0.25 | 1 |
| 1 | 0.87 | .0.89 | 0.95 | 0.9 | 0.81 | 1 |

Table 1. Correct Location Finding Probability Using both TOA and AOA Information. The average values over all sectors are: $P_{lf}$=76%, $P_{alf}$=92%.

| 1 | 2 | 3 | 4 | 5 | 6 | 7 |
|---|---|---|---|---|---|---|
| 0.77 | 0.69 | 0.64 | 0.67 | 0.81 | 0.74 | 0.75 |
| 0.82 | 0.78 | 0.78 | 0.82 | 0.86 | 0.91 | 0.78 |
| 8 | 9 | 10 | 11 | 12 | 13 | 14 |
| 0.54 | 0.87 | 0.78 | 0.73 | 0.69 | 0.68 | 0.87 |
| 0.71 | 0.91 | 0.87 | 0.88 | 0.94 | 0.9 | 0.88 |
| 15 | 16 | 17 | 18 | 19 | 20 | 21 |
| 0.81 | 0.5 | 0.7 | 0.5 | 0.82 | 0.5 | 0.64 |
| 0.92 | 0.66 | 0.75 | 0.72 | 0.84 | 0.57 | 0.73 |
| 22 | 23 | 24 | 25 | 26 | 27 | 28 |
| 0.23 | 0.59 | 0.39 | 0.55 | 0.7 | 0.76 | 0.83 |
| 0.69 | 0.78 | 0.64 | 0.73 | 0.95 | 0.86 | 0.95 |
| 29 | 30 | 31 | 32 | 33 | 34 | 35 |
| 0.66 | 0.58 | 0.58 | 0.55 | 0.69 | 0.78 | 0.59 |
| 0.87 | 0.91 | 0.69 | 0.79 | 0.91 | 0.88 | 0.71 |
| 36 | 37 | 38 | 39 | 40 | 41 | 42 |
| 0.46 | 0.53 | 0.6 | 0.41 | 0.43 | 0.52 | 0.4 |
| 0.62 | 0.67 | 0.71 | 0.72 | 0.73 | 0.88 | 0.62 |
| 43 | 44 | 45 | 46 | 47 | 48 | 49 |
| 0.65 | 0.15 | 0.58 | 0.65 | 0.73 | 0.16 | 0.49 |
| 0.68 | 0.9 | 0.83 | 0.98 | 0.9 | 0.77 | 0.6 |
| 50 | 51 | 52 | 53 | 54 | 55 | 56 |
| 0.39 | 0.67 | 0.64 | 0.58 | 0.51 | 0.49 | 0.78 |
| 0.73 | 0.93 | 0.76 | 0.91 | 0.88 | 0.76 | 1 |

Table 2. Correct Location Finding Probability Using AOA Information Only.
The average values over all sectors are: $P_{lf}$=60%, $P_{alf}$=80%.

| 1 | 2 | 3 | 4 | 5 | 6 | 7 |
|---|---|---|---|---|---|---|
| 0.1 | 0.03 | 0.02 | 0.15 | 0.2 | 0.24 | 0.23 |
| 0.1 | 0.11 | 0.09 | 0.15 | 0.34 | 0.3 | 0.25 |
| 8 | 9 | 10 | 11 | 12 | 13 | 14 |
| 0.22 | 0.24 | 0.12 | 0.02 | 0.52 | 0.18 | 0.21 |
| 0.41 | 0.42 | 0.18 | 0.08 | 0.65 | 0.28 | 0.24 |
| 15 | 16 | 17 | 18 | 19 | 20 | 21 |
| 0.19 | 0.09 | 0.37 | 0.33 | 0.3 | 0.36 | 0.26 |
| 0.29 | 0.31 | 0.42 | 0.45 | 0.49 | 0.4 | 0.39 |
| 22 | 23 | 24 | 25 | 26 | 27 | 28 |
| 0.33 | 0.06 | 0.09 | 0.51 | 0.41 | 0.3 | 0.52 |
| 0.37 | 0.24 | 0.16 | 0.54 | 0.59 | 0.51 | 0.53 |
| 29 | 30 | 31 | 32 | 33 | 34 | 35 |
| 0.54 | 0.53 | 0.32 | 0.62 | 0.63 | 0.41 | 0.58 |
| 0.59 | 0.61 | 0.42 | 0.67 | 0.7 | 0.6 | 0.67 |
| 36 | 37 | 38 | 39 | 40 | 41 | 42 |
| 0.07 | 0.12 | 0.24 | 0.08 | 0.37 | 0.21 | 0.26 |
| 0.13 | 0.28 | 0.32 | 0.28 | 0.72 | 0.49 | 0.54 |
| 43 | 44 | 45 | 46 | 47 | 48 | 49 |
| 0.12 | 0.26 | 0.17 | 0.34 | 0.03 | 0.86 | 0.11 |
| 0.15 | 0.52 | 0.32 | 0.36 | 0.51 | 0.87 | 0.76 |
| 50 | 51 | 52 | 53 | 54 | 55 | 56 |
| 0.06 | 0 | 0 | 0 | 0.09 | 0 | 0 |
| 0.18 | 0.22 | 0.01 | 0 | 0.51 | 0.79 | 0.85 |

Table 3. Correct Location Finding Probability Using TOA Information Only.
The average values over all sectors are: $P_{lf}$=24%, $P_{alf}$=40%.

| 1 | 2 | 3 | 4 | 5 | 6 | 7 |
|---|---|---|---|---|---|---|
| 0.93 | 0.68 | 0.70 | 0.81 | 0.82 | 0.81 | 0.75 |
| 0.93 | 0.81 | 0.90 | 0.92 | 0.95 | 0.91 | 0.8 |
| 8 | 9 | 10 | 11 | 12 | 13 | 14 |
| 0.84 | 0.66 | 0.92 | 0.9 | 0.89 | 0.73 | 0.8 |
| 0.92 | 0.94 | 0.99 | 0.97 | 0.93 | 0.99 | 0.84 |
| 15 | 16 | 17 | 18 | 19 | 20 | 21 |
| 0.87 | 0.74 | 0.8 | 0.79 | 0.87 | 0.69 | 0.74 |
| 0.94 | 0.87 | 0.88 | 0.97 | 0.96 | 0.82 | 0.79 |
| 22 | 23 | 24 | 25 | 26 | 27 | 28 |
| 0.89 | 0.5 | 0.61 | 0.65 | 0.89 | 0.87 | 0.97 |
| 0.94 | 0.91 | 0.75 | 0.75 | 0.94 | 0.99 | 0.99 |
| 29 | 30 | 31 | 32 | 33 | 34 | 35 |
| 0.83 | 0.68 | 0.65 | 0.78 | 0.84 | 0.76 | 0.85 |
| 0.93 | 0.94 | 0.76 | 0.88 | 0.91 | 0.91 | 1 |
| 36 | 37 | 38 | 39 | 40 | 41 | 42 |
| 0.43 | 0.54 | 0.53 | 0.57 | 0.74 | 0.65 | 0.89 |
| 0.57 | 0.86 | 0.77 | 0.73 | 0.79 | 0.89 | 0.92 |
| 43 | 44 | 45 | 46 | 47 | 48 | 49 |
| 0.95 | 0.32 | 0.48 | 0.57 | 0.43 | 0.21 | 0.89 |
| 0.98 | 0.94 | 0.78 | 0.88 | 0.77 | 0.95 | 1 |
| 50 | 51 | 52 | 53 | 54 | 55 | 56 |
| 0.8 | 0.19 | 0.78 | 0.83 | 0.59 | 0.18 | 0.88 |
| 0.92 | 0.72 | 0.79 | 0.92 | 0.89 | 0.72 | 0.93 |

Table 4. Correct Location Finding Probability with Gaussian Random Jitter Applied to TOA and AOA Features in Measured Fingerprints.
The average values over all sectors are: $P_{lf}$=71%, $P_{alf}$=88%.